Published in final edited form as:
Neuron. 2010 December 22; 68(6): 1159–1172. doi:10.1016/j.neuron.2010.11.031.

Role of ACh-GABA co-transmission in detecting image motion and motion direction

Seunghoon Lee[1,2], **Kyongmin Kim**[2], and **Z. Jimmy Zhou**[1,2,3]

[1]Department of Ophthalmology and Visual Science, Yale University School of Medicine, New Haven, Connecticut 06510

[2]Department of Physiology and Biophysics, University of Arkansas for Medical Sciences, Little Rock, Arkansas 72205

[3]Department of Cellular and Molecular Physiology, Yale University School of Medicine, New Haven, Connecticut 06510

Summary

Starburst amacrine cells (SACs) process complex visual signals in the retina using both ACh and GABA, but the synaptic organization and function of ACh-GABA corelease remain unclear. Here, we show that SACs make cholinergic synapses onto On-Off direction-selective ganglion cells (DSGCs) from all directions, but make GABAergic synapses onto DSGCs only from the null direction. ACh and GABA were released differentially in a Ca^{2+} level-specific manner, suggesting the two transmitters were released from different vesicle populations. Despite the symmetric cholinergic connection, the light-evoked cholinergic input to a DSGC, detected at both light onset and offset, was motion- and direction-sensitive. This input was facilitated by two-spot apparent motion in the preferred direction, but supressed in the null direction, presumably by a GABAergic mechnism. The results revealed a new level of synaptic intricacy in the starburst circuit and suggest differential, yet synergistic, roles of ACh-GABA cotransmission in motion sensitivity and direction selectivity.

Introduction

Since the introduction of Dale's principle of “one neuron releases one fast neurotransmitter” (Dale, 1935), an increasing number of exceptions to this rule have been found in many parts of the nervous system (Burnstock, 2004; Jo and Schlichter, 1999; Jonas et al., 1998; Li et al., 2004; Nishimaru et al., 2005; Seal and Edwards, 2006; Tsen et al., 2000; Wojcik et al., 2006), suggesting that co-release of multiple fast neurotransmitters by a single neuron may represent a significant mode of neurotransmission. However, the mechanism, circuitry, and function of co-neurotransmission in the CNS are poorly understood in general. In the vertebrate retina, SACs synthesize and release two classic fast neurotransmitters of opposite excitability, namely ACh and GABA (Brecha et al., 1988; Kosaka et al., 1988; O'Malley and Masland, 1989; Vaney and Young, 1988). These cells exist as two mirror-symmetric populations across the inner plexiform layer (IPL), with the somas of one population

Correspondence: Z. Jimmy Zhou, Ph.D. Department of Ophthalmology and Visual Science Yale University School of Medicine 300 George Street, Suite 8100 New Haven, CT 06511 Tel.: (203) 785-2076 Fax: (203) 785-7401 jimmy.zhou@yale.edu.

(conventional or OFF SACs) located in the inner nuclear layer (INL) and those of the other population (displaced or ON SACs) in the ganglion cell layer (GCL). The processes (dendrites) of SACs have a radially symmetric ("starburst") dendritic morphology and ramify in two narrow substrata of the IPL, where the dendrites of neighboring SACs and DSGCs cofasiculate to form a dense, honeycomb-shaped meshwork (Famiglietti, 1985; Famiglietti, 1992; Famiglietti, 1983; Tauchi and Masland, 1984; Vaney, 1984). This meshwork is well organized and experimentally approachable, offering a unique opportunity for understanding the mechanism, circuitry, and function of neurotransmitter corelease.

SACs are a key component in the direction-selective circuit (Amthor et al., 2002; Fried et al., 2002; Yoshida et al., 2001). Dual recordings demonstrate that SACs release GABA onto DSGCs from the null, but not the preferred, direction (Fried et al., 2002). SAC dendrites also exhibit directional (centrifugally preferred) calcium responses to image movement (Euler et al., 2002; Lee and Zhou, 2006), which have been attributed, at least in part, to the reciprocal GABA release from SACs onto neighboring SACs (Lee and Zhou, 2006, but also see (Hausselt et al., 2007). These findings, together with a large body of evidence that GABA receptor antagonists block direction selectivity, have established that GABA release from SACs plays a critical role in direction selectivity (Demb, 2007; Fried and Masland, 2007; Fried et al., 2002; Taylor and Vaney, 2003; Zhou and Lee, 2008).

In contrast, the synaptic function of ACh release from SACs is poorly understood, due, in part, to the lack of direct detection of cholinergic synaptic transmission in the mature retina. ACh has been suggested to regulate the responsiveness of retinal ganglion cells (Ariel and Daw, 1982a; Schmidt et al., 1987; Vardi et al., 1989) and to play a role in direction selectivity (Masland et al., 1984; Vaney, 1990), especially in response to the movement of complex images (Grzywacz et al., 1998a; Grzywacz et al., 1998b). However, nicotinic antagonists do not block direction selectivity (Ariel and Daw, 1982b; Cohen and Miller, 1995; Kittila and Massey, 1995; Kittila and Massey, 1997). ACh has also been shown to facilitate the responses of DSGCs to image movement, and this facilitation is thought to occur in all directions, at least in the presence of GABA receptor antagonists (Chiao and Masland, 2002; He and Masland, 1997). Nicotinic antagonists (e.g., d-tubocurarine) are known to inhibit the spike response of DSGCs to both light onset and offset (Ariel and Daw, 1982b; Kittila and Massey, 1997). However, d-tubocurarine was reported to reduce the excitatory current input to a DSGC only at the light offset, but not the onset, though GABA receptor blockers could bring out a d-tubocurarine-sensitive component at the light onset (Fried et al., 2005). Curiously, while dual recordings found asymmetric GABAergic transmission between SACs and DSGCs, the same recording did not detect any cholinergic transmission (Fried et al., 2002). This result is puzzling, since DSGCs have been shown anatomically to make direct synapses with SACs (including ON SACs) (Dacheux et al., 2003; Famiglietti, 1992) and are known to express functional nicotinic receptors (Strang et al., 2005), making them the most likely postsynaptic target of cholinergic synaptic interactions in the retina. Because of these inconsistencies, it is important to determine whether ACh functions as a classic fast excitatory neurotransmitter to mediate direct (monosynaptic) transmission between SACs and DSGCs, or it plays mainly a paracrine role to influence the excitability of many ganglion cells without evoking a detectable excitatory postsynaptic current. It is also critical to understand how ACh-GABA co-transmission is regulated at the synaptic level, what synaptic circuits support this co-transmission, and more importantly, how such co-transmission subserves specific visual functions.

This study directly detected ACh-GABA co-transmission from SACs to DSGCs and showed that both ACh and GABA function as classic, fast neurotransmitters at specific synapses between SACs and DSGCs. It characterized both the anatomical connectivity and the functional organization of the cholinergic and GABAergic synapses between SACs and

DSGCs. The study also discovered differential regulations of ACh and GABA releases from SACs, suggesting that the two transmitters are released from two separate vesicle populations. The results revealed a new level of intricacy in the synaptic circuitry and computational capability of neurotransmitter co-transmission and suggested differential, yet synergistic, roles of ACh-GABA corelease in encoding motion sensitivity and direction selectivity.

Results

Cholinergic and GABAergic synaptic connectivity between SACs and DSGCs

To understand the synaptic connectivity between displaced SACs and On-Off DSGCs (henceforth referred to simply as SACs and DSGCs, respectively), we performed paired patch-clamp recordings in the whole-mount rabbit retina aged between postnatal days 17 and 45. A DSGC was first recorded under on-cell loose-patch clamp to determine its preferred and null directions based on the cell's spike responses to a bright bar moving on a dark background in 12 different directions. The receptive field center of the cell was mapped by flashing a stationary spot at various positions in the receptive field, so that the dendritic field, which is known to match closely the receptive field center (Yang and Masland, 1992), could be revealed without the need to examine the dendritic morphology under fluorescence illumination (Fig.1A). Dual whole-cell voltage-clamp recordings were subsequently made from the same DSGC and a neighboring SAC, whose soma was located either within ±10° of the preferred (or null) direction of the DSGC, or perpendicular (90°) to the preferred-null axis (intermediate direction). The dendrites of the SAC were estimated to overlap about half of the DSGC's dendritic field from the preferred, null, or intermediate side (Fig. 1B). Depolarizing the SAC with a series of voltage pulses in 10-mV amplitude increments (from a holding potential of -70 mV) evoked, in the postsynaptic DSGC, inward synaptic currents at -70 mV (near the Cl^- equilibrium potential, E_{Cl}) and outward synaptic currents at 0 mV (near the cation reversal potential, E_{Cat}) (Fig. 1B). The inward currents consisted primarily of an early component with fast rising and decaying kinetics, whereas the outward currents contained both an initial fast component and a sustained component that outlasted the duration of the presynaptic depolarization pulse. The inward current could be blocked by the nicotinic receptor antagonist, hexamethonium (HEX, 200 μM, n=6, Fig. 1C), but not by the $GABA_A$ receptor antagonist, SR95531 (50 μM, n=4, Fig. 1D), or the AMPA/KA receptor antagonist, CNQX (40 μM, n=44), which blocked most of the spontaneous excitatory currents at -70 mV (Fig. 1E). The outward postsynaptic currents could be blocked by SR95531 (50 μM, n=8, Fig. 1C), but not by CNQX (40 μM, n=44, Fig. 1E) or a combination of HEX (200 μM) and CNQX (40 μM, n=4, Fig. 1D). These results demonstrated, at a synaptic level, that SACs released both ACh and GABA onto DSGCs, and that both of these transmitters mediated fast synaptic transmission.

Notably, the maximum amplitude of the nicotinic current in a DSGC (typically evoked by presynaptic depolarization of a SAC from -70 mV to -10 mV or above, Fig. 1B) showed no statistically significant difference, regardless whether the presynaptic SAC was located on the preferred (n=22), null (n=20), or intermediate (n = 4) side of the DSGC (mean ± s.e.m: 183 ± 19, 138 ± 20, and 135 ± 12 pA, respectively; p = 0.22, one-way ANOVA, Fig. 1F). In contrast, the maximum GABA response amplitude in DSGCs (evoked typically by presynaptic depolarization from -70 mV to about -10 mV or above) was significantly smaller for preferred side (34 ± 9 pA, n = 22, Fig. 1F) than for null side (321 ± 28 pA, n = 20, $p<0.01$), and intermediate side (228 ± 35 pA, n = 5, p=0.01) SAC stimulation, though no statistical difference was resolved between the null and intermediate directions (p=0.14) (one-way ANOVA with Games-Howell post hoc test). To rule out the possibility that extrasynaptic spill-over of a large amount of released ACh might lead to similar cholinergic response amplitudes from preferred and null directions, we also compared postsynaptic

responses to a low-level ACh release (evoked by depolarizing the presynaptic SAC to just above the threshold for ACh release). We define first-detectable response as the first postsynaptic response generated by a series of presynaptic depolarizing steps (in 10-mV amplitude increments). The first-detectable nicotinic response (typically evoked by a depolarizing step from -70 to -30 mV), which was much smaller than the maximum response, also showed no statistically significant difference in amplitude among the preferred (n=22), null (n=20), and intermediate (n=4) directions (mean ± s.e.m: 49 ± 6, 50 ± 9, and 41 ± 2 pA, respectively; p = 0.86, one-way ANOVA, Fig. 1H). However, the first-detectable GABA responses were again significantly smaller from the preferred (16 ± 4, n=22) direction than from the null (271 ± 27, n=20, $p<0.01$) and intermediate (189 ± 42 pA, $p < 0.05$, Fig. 1I) directions (one-way ANOVA with Games-Howell post hoc test). The results on GABAergic transmission, obtained from 22 preferred, 20 null, and 4 intermediate pairs of dual recordings, were consistent with, but statistically substantiated, a previous report of a directionally asymmetric GABAergic connectivity between SACs and DSGCs (Fried et al., 2002). On the other hand, the results on cholinergic synaptic transmission between SACs and DSGCs contradicted the previous report which did not detect such a transmission (Fried et al., 2002). It is remarkable that the spatial symmetry of cholinergic and GABAergic synaptic connections between SACs and DSGCs were completely different, suggesting that synaptic connectivity between these two cell types is not based simply on the relative direction of the presynaptic and postsynaptic dendrites. Rather, the synaptic connectivity between SACs and DSGCs is controlled at a much more specific and local level, depending on the identity of the synapses, as well as the direction of the dendrites.

To demonstrate the presence of monosynaptic nicotinic and GABAergic transmissions from a SAC to a neighboring DSGC, we analyzed the synaptic delay of cholinergic and GABAergic transmissions under dual voltage clamp. The temporal delay between the onset of the presynaptic voltage pulse and the onset of postsynaptic current response was 6.61 ± 0.28 ms (mean ± s.e.m, n=18) for cholinergic, and 6.54 ± 0.30 (mean ± s.e.m, n=18) for GABAergic transmission (Fig. 2A, B). A large portion of this delay corresponded to the time required to activate presynaptic Ca^{2+} currents under our recording condition (data not shown) and was similar to some of the synaptic delays previously reported for other CNS synapses (Jo and Schlichter, 1999; Jonas et al., 1998). However, the relative difference in synaptic delay between the cholinergic and GABAergic responses was not statistically distinguishable (p=0.48, Fig. 2C), suggesting that at least the initial GABAergic response was not mediated by polysynaptic transmission activated by cholinergic excitation. The presence of direct ACh-GABA co-transmission between SACs and DSGCs was further proven by uncaging Ca^{2+} from DM-nitrophen (loaded in SACs via the patch electrode) under the condition, in which all potential Ca^{2+}-dependent polysynaptic transmission was blocked by the Ca^{2+} channel blocker Cd^{2+} (300-500 μM). Ca^{2+} uncaging in a single SAC evoked rapid cholinergic and GABAergic responses from a neighboring DSGC (Fig. 2D, E), demonstrating unequivocally ACh-GABA co-transmission between SACs and DSGCs in functionally mature rabbit retina.

Cholinergic contribution to light-evoked synaptic inputs to DSGCs

We next examined cholinergic and GABAergic contributions to the visual responses of DSGCs. A moving light bar elicited directionally asymmetric excitatory (EPSC) and inhibitory (IPSC) postsynaptic currents in DSGCs (Fig. 3A). The IPSCs evoked by the null movement were much larger than those evoked by the preferred movement as previously reported (Fried et al., 2002;Fried et al., 2005;Taylor and Vaney, 2002;Weng et al., 2005), and they were largely blocked by SR95531 (50 μM, n=5, data not shown), consistent with a critical role of asymmetric GABAergic inputs from SACs in direction selectivity (Fried et al., 2002). The light-evoked EPSCs in DSGCs were also highly asymmetric, but in the

opposite direction, namely, larger during preferred than null movement (Fig. 3A), as previously observed (Fried et al., 2002;Fried et al., 2005;Taylor and Vaney, 2002;Weng et al., 2005). Contrary to a previous report (Fried et al., 2005), we found a significant contribution of nicotinic input to both the On (Fig. 3B, left) and Off (Fig. 3B, right) responses of DSGCs to a moving bar, because HEX (200-400 μM) consistently reduced the EPSCs evoked by the leading and the trailing edge of the moving bar (Fig. 3B). The remaining EPSCs were further reduced by the NMDA receptor antagonist, CPP (25 μM), resulting in three separate EPSC components which we term HEX-sensitive, CPP-sensitive and HEX-CPP-insensitive (Fig. 3B). Compared with the CPP-sensitive and HEX-CPP-insensitive components, the HEX-sensitive component seemed to reach its peak amplitude slightly faster and also decayed faster. Among these excitatory input components, the amplitude of HEX-sensitive component was significantly directionally asymmetric ($p<0.01$ for both On and Off responses), and so was the amplitude of the CPP-sensitive component ($p<0.01$ for both On and Off responses) (Fig. 3D). However, the amplitude of the HEX-CPP-insensitive component was not asymmetric ($p=0.22$ for On, and 0.91 for Off responses) (Fig. 3D). The total charge transfer (integral of current response over time, Q) was also directionally asymmetric for the HEX-sensitive component ($p\leq0.01$ for both ON and Off responses) and CPP-sensitive component ($p<0.05$ for both On and OFF responses), but not for the HEX-CPP-insensitive component ($p=0.81$ and 0.50 for On and Off responses, respectively). Similar results were also obtained by applying CPP and HEX in a reverse order (Fig. 3C), which again revealed a directionally asymmetric CPP-sensitive component as measured by the current amplitude ($p<0.01$ for both On and Off responses) and the total charge transfer ($p<0.05$ for both On and Off responses), as well as a directionally asymmetric HEX-sensitive component as measured by the current amplitude ($p<0.01$ for both On and Off responses) and by the total charge transfer ($p<0.01$ for both ON and Off responses). No directional asymmetry was detected for the CPP-HEX-insensitive component ($p=0.064$ and 0.39 for On and Off current response amplitudes, respectively; $p=0.6$ and 0.8 for the On and Off total charge transfer, respectively)

The finding of a cholinergic component in the On response of DSGCs was consistent with the observation of cholinergic transmission between On SACs and DSGCs (Fig.1). However, given that our paired recordings showed no statistically significant asymmetry in cholinergic connectivity between SACs and DSGCs (Fig. 1F,H), it was paradoxical that the HEX-sensitive component in the light response was directionally asymmetric. A possible explanation is that motion-evoked release of ACh from SACs onto DSGCs is *functionally* asymmetric, but the cholinergic synaptic connectivity is *anatomically* symmetric (see below). The finding of directional asymmetry in the NMDA-component, but not the AMPA/KA-component, raised the possibility that the fast, direction-selective nicotinic input might act synergistically with a direction-selective NMDA input to provide an associative excitation that helps the cell overcome the voltage-dependent Mg^{2+} blockade of NMDA receptors during the preferred direction movement (Fig. S1). However, the difference in direction selectivity between NMDA and AMPA/KA components remains to be understood.

Receptive field structure of the cholinergic input to DSGCs

In addition to the opposite directional asymmetry, the light-evoked GABAergic input and the HEX-sensitive input to a DSGC also differ dramatically in spatial extent. The GABAergic input could be evoked from the null side when the leading edge of a moving bar was as far as 150 μm (ranging 30 to 150 μm, with a mean ± sd of 64 ± 39 μm, n = 53) from the edge of the DSGC's dendritic field (Fig. 3A), consistent with it being a leading lateral inhibition from SACs (Fried et al., 2002). In contrast, the excitatory inputs, including the HEX-sensitive input, were restricted within the dendritic field of the DSGC (n = 12, Fig.

3A), as previously reported (Fried et al., 2002;Fried et al., 2005;Taylor and Vaney, 2002;Yang and Masland, 1992;Yang and Masland, 1994).

To understand the spatial properties of the cholinergic receptive field (RF) of a DSGC, a two-spot apparent motion paradigm was used. Flashing a stationary light spot in the RF surround could not evoke a detectable HEX-sensitive EPSC (Fig. 4A), suggesting that the nicotinic inputs formed a "silent" excitatory surround, which did not produce a leading lateral excitation during stimulus movement. This result is consistent with a previous report that the OFF cholinergic input to DGGC also does not show an extended surround (Fried et al., 2005). However, when two stationary spots were flashed in a quick succession to simulate a preferred-direction movement, the first flash (in RF surround, which by itself did not evoke a cholinergic response) greatly facilitated the HEX-sensitive response to the second flash (in RF center, Fig. 4A, B), indicating that ACh release was facilitated by stimulus motion. This new finding provided a synaptic basis for the suggestion that ACh facilitates motion detection (Chiao and Masland, 2002;He and Masland, 1997). Notably, however, when two-spot flashes were given to simulate a null-direction motion, the HEX-sensitive response to the second flash was not facilitated, but suppressed (Fig. 4A, B), indicating that motion facilitation in DSGCs was directionally selective, consistent with the above result that the HEX-sensitive response was smaller during null movement than preferred movement (Fig. 3B-D). Since the cholinergic synaptic connectivity between SACs and DSGCs was spatially symmetric (Fig. 1F, H), the directional facilitation of the cholinergic input to a DSGC was unexpected. It was also contrary to a previous conclusion that ACh facilitates motion sensitivity non-directionally (Chiao and Masland, 2002;He and Masland, 1997). Because the non-directional motion facilitation by ACh is shown mostly in the presence of GABA receptor antagonists (Chiao and Masland, 2002;He and Masland, 1997), our results suggest that a new level of GABAergic inhibition was involved in suppressing ACh facilitation from the null direction (see Discussion). Indeed, when $GABA_A$ receptors were blocked by SR95531 (50 μM, n=4), the nicotinic input to a DSGC during moving bar stimulation became directionally symmetric (Fig. S2, also see Fried et al., 2005).

Differential regulation of ACh and GABA corelease from SACs

The "silent" nature of the cholinergic surround may have a distinct advantage in preserving the spatial resolution of a DSGC, because it prevents the expansion of the RF center by the surround excitation. However, why is the cholinergic lateral excitation "silent", while the GABAergic lateral inhibition from the same SAC is not? We found that the Ca^{2+} channel blocker Cd^{2+} (300 μM), or nominally free extracellular Ca^{2+} ($[Ca^{2+}]_o = 0$), abolished both nicotinic and GABAergic transmissions between SACs and DSGCs (Fig. 5D,E), indicating that both ACh and GABA releases were triggered by extracellular Ca^{2+} entry through voltage-gated Ca^{2+} channels. Surprisingly, however, reducing $[Ca^{2+}]_o$ from 1.5 to 0.2 mMEq nearly abolished the nicotinic transmission (even in the presence of 4 μM neostigmine, an acetylcholine esterase inhibitor, n=3, data not shown), while a significant portion of the GABAergic transmission still remained (Fig. 5A-C, E). The voltage (presynaptic)-response (postsynaptic) curve showed a blockade of nicotinic responses at all presynaptic depolarization potentials in 0.2 mMEq $[Ca^{2+}]_{o,}$ whereas the GABA response curve was shifted toward a more positive depolarization potential by about 10 mV (Fig. 5B). The results showed that ACh release required a higher $[Ca^{2+}]_o$ than did GABA release. Pair-pulse stimulation further showed that the cholinergic, but not the GABAergic, transmission was facilitated strongly by repetitive stimulation (Fig. 5F, G), suggesting a role of cumulative excitation in ACh release. These results demonstrate an intrinsic difference in ACh and GABA releases from SACs, providing an important explanation for the different spatial properties (silent vs. leading) of the cholinergic and GABAergic inputs to DSGCs (see discussion).

To find further evidence that ACh and GABA releases from SACs are regulated differentially, we investigated the role of N- and P/Q-type Ca^{2+} channels, the major Ca^{2+} channel subtypes in SACs (Cohen, 2001; Kaneda et al., 2007), in ACh-GABA co-release. The N-type channel blocker, ω-conotoxin GVIA (CTX, 1 μM), nearly completely blocked the nicotinic transmission, but it reduced the initial peak GABAergic transmission only by ~33% (Fig. 6A). On the other hand, the P/Q type channel blocker ω-agatoxin IVA (AgTX, 500 nM) had a larger effect on the GABAergic transmission (blocking ~55% of the initial peak transmission) than did CTX, but it had a much smaller effect on the nicotinic transmission (reducing, but not abolishing, the peak response by ~40%) than did CTX (Fig. 6B-D). These results indicate that the contributions of N and P/Q channels to ACh release were very different from those to GABA release, though the detailed roles of specific Ca^{2+} channels subtypes in ACh and GABA releases remain to be elucidated. Taken together, the above results suggest that ACh and GABA releases from SACs are regulated differentially, providing evidence that ACh and GABA were released from two different populations of synaptic vesicles (see Discussion).

Discussion

The present study demonstrated that ACh and GABA were coreleased from SACs to mediate fast synaptic transmission in two distinct synaptic circuits. The release of the two transmitters was regulated differentially and presumably from two different vesicle populations. The ACh release required higher extracellular Ca^{2+} and repetitive excitation, forming a “silent” and facilitating surround that enables a DSGC to encode motion sensitivity without compromising spatial resolution. In contrast, the GABA release required lower extracellular Ca^{2+} and was less sensitive to repetitive stimulation, forming a reliable and spatially extended (leading) inhibition which, together with asymmetric GABAergic connectivity between SACs and DSGCs, ensures robust direction selectivity. The motion-sensitive cholinergic transmission to a DSGC was suppressed in the null direction, resulting in a functionally asymmetric cholinergic excitation which, in turn, enhances direction selectivity. Together, these findings resulted in an integrated model of ACh-GABA co-transmission and motion-direction co-detection (Fig. 7, see below for detail).

Cholinergic synaptic transmission between SACs and DSGCs

Although ACh release in the retina has been studied with radioactive isotopes since 1970's (Masland and Ames, 1976; Masland and Mills, 1979; Massey and Neal, 1979a; Massey and Neal, 1979b), the synaptic mechanism and synaptic circuitry of cholinergic transmission have remained poorly understood. Our dual patch-clamp recordings from SACs and DSGCs now clearly detected fast nicotinic synaptic transmission, which consisted of a fast initial peak component, followed by a much smaller and prolonged/slow component (Fig. 1). The fast nicotinic component was found reliably in >90% of the pair recordings (>60 pairs in various directions), demonstrating the presence of classic fast nicotinic transmission at SAC-DSGC synapses. Statistical analysis of our dual recording data suggested directionally symmetric cholinergic synaptic connectivity between SACs and DSGCs. A HEX-sensitive cholinergic EPSC was also detected in DSGCs in response to both the leading and the trailing edge of a moving light stimulus. Curiously, however, the light-evoked, HEX-sensitive EPSC in the DSGC was spatially asymmetric (larger from the preferred direction than from the null direction, Fig.3), as reported for the OFF response (Fried et al., 2005). Since the cholinergic input to a DSGC was suppressed during null apparent motion (Fig. 4), and since both the cholinergic facilitation of DSGC responses to motion and the cholinergic response of a DSGC to stationary light stimulation are non-directional in the presence of GABAergic antagonists (Fig. S2, also see Chiao and Masland, 2002, Fried et al., 2005, and He and Mansland, 1997), it is plausible that a strong asymmetric GABAergic inhibition is

present upstream of the ACh release sites, which suppresses ACh release onto a DSGC from the null direction, but spares the release from the preferred direction. This asymmetric GABAergic inhibition may act directly and selectively on the cholinergic synapses between SACs and DSGCs in the null direction (e.g., via selective GABAergic synapses among neighboring SACs, Fig. 7C). Alternatively, because the CPP-sensitive NMDA input and the HEX-sensitive cholinergic input to a DSGC were both suppressed in the null direction to a similar degree (Fig. 3D), the asymmetric GABAergic inhibition may act on bipolar cells, in such a way that local glutamate inputs to the ACh release sites on a SAC dendrite are already directionally asymmetric, depending on whether the cholinergic synapses are made onto a DSGC in the preferred, or the null direction (Fig. 7C). In either scenario, a previously unappreciated level of selectivity and complexity must exist in SAC dendrites, where semi-independent signal processing occurs locally—not only at the level of electrotonically isolated sections of the distal dendrites as previously thought, but also at the level of individual synapses. Local processing at individual synapses would allow the same centrifugal motion to facilitate one population of cholinergic output synapses (made onto DSGCs along the preferred direction), but to suppress another population of cholinergic output synapses (made onto DSGCs along the null direction), so that directional cholinergic facilitation can be produced. Given the existence of remarkable selectivity in GABAergic connectivity between SACs and DSGCs (Fig. 1, also see Fried et al., 2002), such an intricate synaptic organization in the SAC network is conceivable. It is yet to be determined whether a centripetally moving light bar would suppress all cholinergic output synapses as it does to all the GABAergic synapses on a SAC, or it would suppress only one subset of cholinergic synapses (made onto DSGCs along the preferred direction), but not the other set (made onto DSGCs along the null direction).

The integration of directional cholinergic facilitation with directional GABAergic inhibition shown in Fig. 7 produces a push-pull mechanism for direction selectivity. The overall outcome of this mechanism bears some similarity to the push-pull cotransmission model of direction selectivity (Vaney, 1990;Vaney and Taylor, 2002), though the actual synaptic organization hypothesized in the cotransmission model is quite different from that found in the present study. While the directional cholinergic enhancement of DSGC light responses does not dramatically increase the direction selective index because null-direction responses are already at the minimum due to inhibition (He and Masland, 1997), the dramatic increase in spikes by cholinergic facilitation, especially at the onset of the response to preferred-direction movement, may enhance the motion and directional information conveyed to the brain by a DSGC.

It should be pointed out that, although HEX was applied to the entire retina in our experiments, the HEX-sensitive EPSC component recorded from DSGCs was likely mediated predominantly by nicotinic receptors present directly on DSGCs for the following reasons. (1) Our dual recordings clearly demonstrates a direct nicotinic synaptic input from SACs to DSGCs, consistent with previous anatomical evidence that SACs make numerous contacts with DSGCs (Dacheux et al., 2003; Famiglietti, 1992; Vaney, 1994). (2) DSGCs are known to express nicotinic receptors (Strang et al., 2005) and to give robust, direct responses to nicotinic agonists (data not shown), whereas SACs (Zheng et al., 2004; Zhou and Fain, 1995) and bipolar cells (T. Mon and Z.J. Zhou, unpublished observation) give little or no response to exogenous nicotinic agonists in the mature rabbit retina. (3) It is possible that some other amacrine cells express nicotinic receptors, and that their feedback inhibition onto bipolar cells may be affected by HEX, resulting in a change (e.g., an enhancement) in glutamatergic EPSCs in the DSGC. However, even when the majority of the glutamatergic EPSCs in the DSGC was blocked by CPP, subsequent application of HEX still revealed a similar, directionally selective HEX-sensitive EPSC component in DSGCs

(Fig. 3C, D), suggesting that the majority of the HEX-sensitive EPSC component detected under our recording condition was a direct nicotinic input to the DSGC.

GABAergic synaptic transmission between SACs and DSGCs

Our dual patch-clamp recordings demonstrated that GABAergic transmission between SACs and DSGCs occurred only from the null, but not from the preferred direction. This asymmetric GABAergic transmission directly contributed to the asymmetric light-evoked inhibitory inputs to DSGCs. Contrary to the facilitatory, motion-sensitive cholinergic transmission, the GABAergic transmission was hardly affected by repetitive stimulation, consistent with the previous finding that apparent motion did not alter GABA release from SACs located in the null direction (Fried et al., 2005). Such a reliable, spatially extended, and asymmetric GABAergic inhibition would ensure robust direction selectivity under a wide variety of stimulation conditions.

Our conclusion of an asymmetric GABAergic transmission from SACs to DSGCs is consistent with a previous report (Fried et al., 2002), which first made this landmark discovery. However, several detailed differences between the current and previous report are worth pointing out. (1) Our conclusions were drawn from over 20 pairs of preferred-direction and 20 pairs of null-direction recordings, as opposed to the 3 preferred pairs and the 3 null pairs of recordings reported previously. Thus, the present results greatly enhanced the confidence level of this important conclusion. (2) In the present study, the asymmetric GABAergic transmission was detected in the same paired recordings that also demonstrated symmetric cholinergic transmission. This result contrasts the previous recordings which found only GABAergic, but not cholinergic, transmission. With the cholinergic currents serving as a control (especially in preferred-direction pairs), our results now ruled out the possibility that the previously reported lack of GABAergic transmission from the preferred direction was due to limited sensitivity of the measurement and/or a small sample size. (3) The maximum amplitude of GABAergic postsynaptic currents reported previously is about 50 pA, whereas the amplitude shown by the present study was typically 300 pA. Also, the GABA currents evoked by our dual recording showed a fast peak response, followed by a more sustained component. This response profile was similar to that of the GABAergic input to a DSGC (Fried et al., 2005) or a SAC (Lee and Zhou, 2006) during a flash of stationary light stimulation. However, the GABAergic currents seen in the previous dual recordings (Fried et al., 2002) show only a delayed peak, which we saw only in a low $[Ca^{2+}]_o$, suggesting that the SACs might not have been optimally stimulated and/or maintained in the previous recordings. We found that it was more difficult to achieve an ideal seal resistance and voltage clamp in older rabbit retinal wholemounts. This might explain why the previous double patch recordings did not resolve the cholinergic transmission between SACs and DSGCs even though GABA responses were detected (Fried et al., 2002), because ACh release requires more Ca^{2+} entry. We believe our results obtained from 17-45 days old rabbits represent the mature function of the starburst and DSGC network, because the mechanism of direction selectivity has been shown to be functionally mature shortly after eye opening (P11 in rabbit) (Chan and Chiao, 2008; Chen et al., 2009; Elstrott et al., 2008; Zhou and Lee, 2005), and it has been reported that the organization of rabbit ganglion cell receptive fields is essentially indistinguishable from adult by P20 (Masland, 1977).

Differential regulation of Ca^{2+}-dependent ACh-GABA corelease

Our finding of the differential regulation of cholinergic and GABAergic synaptic transmissions in SACs was consistent with a previous autoradiographic result that a low $[Ca]_o$ (~0.2 mMEq) abolishes ACh release, but not GABA release (O'Malley and Masland, 1989). Furthermore, our results demonstrate that even in low $[Ca]_o$, the release of GABA

was still mediated by a Ca^{2+}-dependent vesicular mechanism, not a Ca^{2+}-independent GABA transporter mechanism (though our data do not exclude the possibility that there might be additional transporter-mediated GABA releases that are not detectable between SAC and GSDC under dual patch clamp). The different $[Ca^{2+}]_o$-dependence between the cholinergic and GABAergic transmissions may reflect differences in the presynaptic release mechanism, such as the involvement and the location of various Ca^{2+} channel subtypes and intracellular Ca^{2+} sources near the active zone and the local interactions between Ca^{2+} and the exocytotic machinery. We found that N and P/Q Ca^{2+} channel types contributed differentially to various kinetic components of the cholinergic and GABAergic transmission, consistent with a previous report that specific Ca^{2+} channel subtypes have different effects on direction selectivity (Jensen, 1995).

Consistent with a higher demand on $[Ca^{2+}]_o$ for the cholinergic than that for the GABAergic transmission, repetitive stimulation resulted in a strong facilitation of the cholinergic transmission, while the GABAergic transmission showed little facilitation. It has been reported that synapses with a high initial release often display a weak facilitation by repetitive stimulation, thus supplying less dynamic but high fidelity synaptic information, whereas synapses with a low initial release frequently show a strong facilitation, thus providing more dynamic but low fidelity synaptic information (Atwood and Karunanithi, 2002; Blitz et al., 2004; von Gersdorff and Borst, 2002; Zucker and Regehr, 2002). It appears that the GABAergic transmission from SACs to DSGCs may resemble the former case, while the cholinergic transmission may be similar to the latter case. This intrinsic difference in the synaptic efficacy may explain, in part, why GABA release from the distal dendrites of a SAC could be reliably triggered by a light stimulus located at the proximal dendrites (thus providing a reliable, leading surround inhibition for robust direction selectivity), whereas ACh release occurred only when the stimulus reached the release sites (hence, forming a “silent” surround), and predominantly when the stimulus was moving centrifugally (hence, producing motion-sensitivity). However, intrinsic synaptic properties alone are not sufficient to account for the different spatiotemporal profiles of cholinergic and GABAergic transmission, because blocking GABAergic inhibition brought out the surround ACh excitation and dramatically alter the ACh release profile (Fig. S2) (Chiao and Masland, 2002; Fried et al., 2005; He and Masland, 1997). It is the intricate combination of intrinsic properties and network regulation, particularly a selective GABAergic inhibition, that shapes the release of ACh.

Possibility of two different populations of synaptic vesicles for ACh and GABA releases

The present study has established that both ACh and GABA are released by SACs in a Ca^{2+}-dependent manner, suggesting a vesicular release mechanism. So far, there has been no definitive anatomical data that would differentiate whether ACh and GABA are released from the same or different vesicle populations. This study provided first strong functional evidence that ACh and GABA are released from two different vesicle populations. Lowering $[Ca^{2+}]_o$ to 0.2 mMEq completely blocked cholinergic transmission but spared GABAergic transmission, suggesting that only GABA, but not ACh, was released under this condition. One might argue that ACh could still be released together with GABA from the same vesicles in 0.2 mMEq $[Ca^{2+}]_o$, and that, because less vesicles were released under this condition, ACh was no longer detectable by the postsynaptic nicotinic receptors, though GABA remained detectable by the postsynaptic GABA receptors (for reasons such as GABA receptors being closer to the release site). If this were the case, then preventing ACh degradation in the synaptic cleft by the application of acetylcholine esterase inhibitor (neostigmine) would be expected to restore some cholinergic transmission in the low $[Ca^{2+}]_o$ medium. However, our experiments found no evidence for such a neostigmine effect (data not shown), supporting the conclusion that ACh was released separately from GABA.

It remains to be understood whether ACh- and GABA-containing vesicles are released from the same or different varicosities (or dendritic release zones), and whether the cholinergic and GABAergic synapses between SACs and DSGCs share a similar anatomical structure.

Implication of ACh-GABA cotransmission in neuronal computation

Complex neuronal computation is often thought to be mediated by complicated neuronal interactions involving many different cell types and even different areas of the brain. In the retina, direction and motion sensitivity represent a kind of neuronal computation that involves only a small number of cell types. In this case, the computational complexity seems to be achieved not by a complex assortment of many different cell types, but rather by sophisticated synaptic connections and intricate regulations of synaptic interactions among a limited number of cell types in the network. A key player in this network is the SAC. Our results suggest that ACh-GABA corelease enables the starburst circuit to encode both motion sensitivity and direction selectivity, thereby reducing the number of retinal circuits and circuit components required for the computation of these two visual cues. Although detailed synaptic mechanisms remain to be elucidated, the results from this study revealed a previously unappreciated level of intricacy in both synaptic connectivity and synaptic regulation of the starburst network that may have important implications for retinal processing in particular and neuronal computation in general.

Experimental Procedures

Retinas were dissected under dim red illumination from eyes of postnatal day 17-45 New Zealand White rabbits immediately following euthanization by an overdose of sodium pentobarbital (200 mg/kg, i.v.) according to an IACUC approved protocol. Patch-clamp recordings were made from SACs and DSGCs in flatmount retina in Ames medium (Sigma-Aldrich, Saint Louis, MO), equilibrated with 95% O_2 and 5% CO_2) at ~35°C as described previously (Lee and Zhou, 2006; Zheng et al., 2004; Zhou and Fain, 1995). Spike responses of DSGCs were recorded with an on-cell loose-patch electrode (3-5 MΩ, filled with Ames medium). Whole-cell patch clamp was made from SACs using a pipette solution containing (in mM) 110 $CsMeSO_4$, 15 CsOH, 5 NaCl, 0.5 $CaCl_2$, 2 $MgCl_2$, 5 EGTA, 2 adenosine 5'-triphosphate (disodium salt), 0.5 guanosine 5'-triphosphate (trisodium salt), 10 HEPES, and 2 ascorbate (pH 7.2). The same pipette solution, supplemented with 10 mM lidocaine N-ethyl bromide (QX314), was used for whole-cell recording from DSGCs. Lucifer yellow (0.1-0.3%, w/v) was included in the whole-cell pipette solution for morphological confirmation of cell types. The effects of Ca^{2+} channel blockers, ω-conotoxin GVIA and ω-agatoxin IVA, which had a slow onset, were tested under perforated patch-clamp recording from SACs using electrodes (6-8 MΩ) filled with (in mM) 145 glutamic acid, 10 HEPES, 10 NaCl, and 500 μg/ml amphotericin B (titrated to pH 7.2 with 147 mM CsOH). Lysozyme (1.5 mg/ml) was added to the superfusate to prevent nonspecific binding of calcium channel toxins to the perfusion system.

Flash photolysis of caged Ca^{2+} (DM-nitorphen) in SACs was done under dual whole-cell voltage-clamp recordings from pairs of SACs and DSGCs, with the pipette solution for SAC recording containing (in mM) 95 $CsMeSO_4$, 30 CsOH, 5 NaCl, 2 $CaCl_2$, 6 $Ca(NO_3)_2$, 2 adenosine 5'-triphosphate (disodium salt), 0.5 guanosine 5'-triphosphate (trisodium salt), 40 HEPES, 2 ascorbate, and 10 DM-nitrophen (pH 7.2). DM-nitrophen was allowed to diffuse into the SAC for 5-7 min before a UV light (355 nm in wavelength, 25 ms in duration) was flashed onto the SAC dendrites. The UV light was generated by a UV laser (30 mW average output power, 3 μJ/pulse at 10kHz, Model DPSL355/30, Rapp Opto Electronik, Heidelberg, Germany), which was guided to the epi-fluorescence port of the microscope via a spot illumination adaptor (OSI BX, Rapp Opto) by a quartz optic fiber (940 μm in diameter) and focused in a 50-μm-diameter spot on the SAC dendrites via a 60× objective lens (NA/09).

The uncaging area was positioned by moving the microscope stage, on which the recording chamber and micromanipulators were mounted.

To isolate the various pharmacological components of the light response of a DSGC (Fig. 3B-D, raw response traces recorded under each pharmacological condition were averaged over at least two trials to find the mean and variance at the peak response. After the averaged traces were subtracted to isolate individual pharmacological components, the variances were propagated according to $\sigma_{a-b}^2 = \sigma_a^2 + \sigma_b^2$. The propagated variance of each component was then pooled from all the cells tested to calculate the pooled variance (weighted sum of variance), which was then used for statistical analysis. Results were expressed as mean ± s.e.m., and the statistical significance was determined at the level of α=0.05 by two-tailed Student's *t*-test (Fig. 3) or ANOVA (together with Games-Howell post hoc test, if homoscedasticity was not satisfied).

Additional information about patch-clamp recording, light stimulation, and data analysis can be found in Supplemental Experimental Procedures.

Supplementary Material

Refer to Web version on PubMed Central for supplementary material.

Acknowledgments

This work was supported in part by NIH grants R01EY017353 and R01EY10894 (ZJZ), Departmental Challenge Grant from Research to Prevent Blindness, Inc. and NIH Vision Core Grant (P30 EY000785).

References

Amthor FR, Keyser KT, Dmitrieva NA. Effects of the destruction of starburst-cholinergic amacrine cells by the toxin AF64A on rabbit retinal directional selectivity. Vis Neurosci. 2002; 19:495–509. [PubMed: 12511082]

Ariel M, Daw NW. Effects of cholinergic drugs on receptive field properties of rabbit retinal ganglion cells. J Physiol (Lond). 1982a; 324:135–160. [PubMed: 7097593]

Ariel M, Daw NW. Pharmacological analysis of directionally sensitive rabbit retinal ganglion cells. J Physiol (Lond). 1982b; 324:161–185. [PubMed: 7097594]

Atwood HL, Karunanithi S. Diversification of synaptic strength: presynaptic elements. Nat Rev Neurosci. 2002; 3:497–516. [PubMed: 12094207]

Blitz DM, Foster KA, Regehr WG. Short-term synaptic plasticity: a comparison of two synapses. Nat Rev Neurosci. 2004; 5:630–640. [PubMed: 15263893]

Brecha N, Johnson D, Peichl L, Wassle H. Cholinergic amacrine cells of the rabbit retina contain glutamate decarboxylase and gamma-aminobutyrate immunoreactivity. Proc Natl Acad Sci U S A. 1988; 85:6187–6191. [PubMed: 3413087]

Burnstock G. Cotransmission. Curr Opin Pharmacol. 2004; 4:47–52. [PubMed: 15018838]

Chan YC, Chiao CC. Effect of visual experience on the maturation of ON-OFF direction selective ganglion cells in the rabbit retina. Vision Res. 2008; 48:2466–2475. [PubMed: 18782584]

Chen M, Weng S, Deng Q, Xu Z, He S. Physiological properties of direction-selective ganglion cells in early postnatal and adult mouse retina. J Physiol. 2009; 587:819–828. [PubMed: 19103682]

Chiao CC, Masland RH. Starburst cells nondirectionally facilitate the responses of direction-selective retinal ganglion cells. J Neurosci. 2002; 22:10509–10513. [PubMed: 12486140]

Cohen ED. Voltage-gated calcium and sodium currents of starburst amacrine cells in the rabbit retina. Vis Neurosci. 2001; 18:799–809. [PubMed: 11925015]

Cohen ED, Miller RF. Quinoxalines block the mechanism of directional selectivity in ganglion cells of the rabbit retina. Proc Natl Acad Sci U S A. 1995; 92:1127–1131. [PubMed: 7862647]

Dacheux RF, Chimento MF, Amthor FR. Synaptic input to the on-off directionally selective ganglion cell in the rabbit retina. J Comp Neurol. 2003; 456:267–278. [PubMed: 12528191]

Dale H. Pharmacology and nerve-endings. Proc R Soc Med (Lond). 1935; 28:319–332.

Demb JB. Cellular mechanisms for direction selectivity in the retina. Neuron. 2007; 55:179–186. [PubMed: 17640521]

Elstrott J, Anishchenko A, Greschner M, Sher A, Litke AM, Chichilnisky EJ, Feller MB. Direction selectivity in the retina is established independent of visual experience and cholinergic retinal waves. Neuron. 2008; 58:499–506. [PubMed: 18498732]

Euler T, Detwiler PB, Denk W. Directionally selective calcium signals in dendrites of starburst amacrine cells. Nature. 2002; 418:845–852. [PubMed: 12192402]

Famiglietti EV. Starburst amacrine cells: morphological constancy and systematic variation in the anisotropic field of rabbit retinal neurons. J Neurosci. 1985; 5:562–577. [PubMed: 3973684]

Famiglietti EV. Dendritic co-stratification of ON and ON-OFF directionally selective ganglion cells with starburst amacrine cells in rabbit retina. J Comp Neurol. 1992; 324:322–335. [PubMed: 1383291]

Famiglietti EV Jr. 'Starburst' amacrine cells and cholinergic neurons: mirror-symmetric on and off amacrine cells of rabbit retina. Brain Res. 1983; 261:138–144. [PubMed: 6301622]

Fried SI, Masland RH. Image processing: how the retina detects the direction of image motion. Curr Biol. 2007; 17:R63–66. [PubMed: 17240332]

Fried SI, Munch TA, Werblin FS. Mechanisms and circuitry underlying directional selectivity in the retina. Nature. 2002; 420:411–414. [PubMed: 12459782]

Fried SI, Munch TA, Werblin FS. Directional selectivity is formed at multiple levels by laterally offset inhibition in the rabbit retina. Neuron. 2005; 46:117–127. [PubMed: 15820698]

Grzywacz NM, Amthor FR, Merwine DK. Necessity of acetylcholine for retinal directionally selective responses to drifting gratings in rabbit. J Physiol. 1998a; 512(Pt 2):575–581. [PubMed: 9763645]

Grzywacz NM, Merwine DK, Amthor FR. Complementary roles of two excitatory pathways in retinal directional selectivity. Vis Neurosci. 1998b; 15:1119–1127. [PubMed: 9839976]

Hausselt SE, Euler T, Detwiler PB, Denk W. A dendrite-autonomous mechanism for direction selectivity in retinal starburst amacrine cells. PLoS Biol. 2007; 5:e185. [PubMed: 17622194]

He S, Masland RH. Retinal direction selectivity after targeted laser ablation of starburst amacrine cells. Nature. 1997; 389:378–382. [PubMed: 9311778]

Jensen RJ. Effects of Ca2+ channel blockers on directional selectivity of rabbit retinal ganglion cells. J Neurophysiol. 1995; 74:12–23. [PubMed: 7472316]

Jo YH, Schlichter R. Synaptic corelease of ATP and GABA in cultured spinal neurons. Nat Neurosci. 1999; 2:241–245. [PubMed: 10195216]

Jonas P, Bischofberger J, Sandkuhler J. Corelease of two fast neurotransmitters at a central synapse. Science. 1998; 281:419–424. [PubMed: 9665886]

Kaneda M, Ito K, Morishima Y, Shigematsu Y, Shimoda Y. Characterization of voltage-gated ionic channels in cholinergic amacrine cells in the mouse retina. J Neurophysiol. 2007; 97:4225–4234. [PubMed: 17428902]

Kittila CA, Massey SC. Effect of ON pathway blockade on directional selectivity in the rabbit retina. J Neurophysiol. 1995; 73:703–712. [PubMed: 7760129]

Kittila CA, Massey SC. Pharmacology of directionally selective ganglion cells in the rabbit retina. J Neurophysiol. 1997; 77:675–689. [PubMed: 9065840]

Kosaka T, Tauchi M, Dahl JL. Cholinergic neurons containing GABA-like and/or glutamic acid decarboxylase-like immunoreactivities in various brain regions of the rat. Exp Brain Res. 1988; 70:605–617. [PubMed: 3384059]

Lee S, Zhou ZJ. The synaptic mechanism of direction selectivity in distal processes of starburst amacrine cells. Neuron. 2006; 51:787–799. [PubMed: 16982423]

Li WC, Soffe SR, Roberts A. Glutamate and acetylcholine corelease at developing synapses. Proc Natl Acad Sci U S A. 2004; 101:15488–15493. [PubMed: 15494439]

Masland RH. Maturation of function in the developing rabbit retina. J Comp Neurol. 1977; 175:275–286. [PubMed: 903424]

Masland RH, Ames A. d. Responses to acetylcholine of ganglion cells in an isolated mammalian retina. J Neurophysiol. 1976; 39:1220–1235. [PubMed: 993829]

Masland RH, Mills JW. Autoradiographic identification of acetylcholine in the rabbit retina. J Cell Biol. 1979; 83:159–178. [PubMed: 92476]

Masland RH, Mills JW, Cassidy C. The functions of acetylcholine in the rabbit retina. Proc R Soc Lond B Biol Sci. 1984; 223:121–139. [PubMed: 6151181]

Massey SC, Neal MJ. The light evoked release of acetylcholine from the rabbit retina iN vivo and its inhibition by gamma-aminobutyric acid. J Neurochem. 1979a; 32:1327–1329. [PubMed: 430091]

Massey SC, Neal MJ. Release of [3H]-acetylcholine from the isolated retina of the rat by potassium depolarization: dependence on high affinity choline uptake. Br J Pharmacol. 1979b; 65:271–276. [PubMed: 760901]

Nishimaru H, Restrepo CE, Ryge J, Yanagawa Y, Kiehn O. Mammalian motor neurons corelease glutamate and acetylcholine at central synapses. Proc Natl Acad Sci U S A. 2005; 102:5245–5249. [PubMed: 15781854]

O'Malley DM, Masland RH. Co-release of acetylcholine and gamma-aminobutyric acid by a retinal neuron. Proc Natl Acad Sci U S A. 1989; 86:3414–3418. [PubMed: 2566171]

Schmidt M, Humphrey MF, Wassle H. Action and localization of acetylcholine in the cat retina. J Neurophysiol. 1987; 58:997–1015. [PubMed: 3694255]

Seal RP, Edwards RH. Functional implications of neurotransmitter co-release: glutamate and GABA share the load. Curr Opin Pharmacol. 2006; 6:114–119. [PubMed: 16359920]

Strang CE, Andison ME, Amthor FR, Keyser KT. Directionally Selective Ganglion Cells in Rabbit Retina Express Functional A7 nAChRs. Invest Ophthalmol Vis Sci. 2005; 46:2243.

Tauchi M, Masland RH. The shape and arrangement of the cholinergic neurons in the rabbit retina. Proc R Soc Lond B Biol Sci. 1984; 223:101–119. [PubMed: 6151180]

Taylor WR, Vaney DI. Diverse synaptic mechanisms generate direction selectivity in the rabbit retina. J Neurosci. 2002; 22:7712–7720. [PubMed: 12196594]

Taylor WR, Vaney DI. New directions in retinal research. Trends Neurosci. 2003; 26:379–385. [PubMed: 12850434]

Tsen G, Williams B, Allaire P, Zhou YD, Ikonomov O, Kondova I, Jacob MH. Receptors with opposing functions are in postsynaptic microdomains under one presynaptic terminal. Nat Neurosci. 2000; 3:126–132. [PubMed: 10649567]

Vaney DI. ‘Coronate’ amacrine cells in the rabbit retina have the ‘starburst’ dendritic morphology. Proc R Soc Lond B Biol Sci. 1984; 220:501–508. [PubMed: 6142459]

Vaney DI. The mosaic of amacrine cells in the mammalian retina. Progressive Retinal Research. 1990; 9:49–100.

Vaney DI. Territorial organization of direction-selective ganglion cells in rabbit retina. J Neurosci. 1994; 14:6301–6316. [PubMed: 7965037]

Vaney DI, Taylor WR. Direction selectivity in the retina. Curr Opin Neurobiol. 2002; 12:405–410. [PubMed: 12139988]

Vaney DI, Young HM. GABA-like immunoreactivity in cholinergic amacrine cells of the rabbit retina. Brain Res. 1988; 438:369–373. [PubMed: 3345446]

Vardi N, Masarachia PJ, Sterling P. Structure of the starburst amacrine network in the cat retina and its association with alpha ganglion cells. J Comp Neurol. 1989; 288:601–611. [PubMed: 2808752]

von Gersdorff H, Borst JG. Short-term plasticity at the calyx of held. Nat Rev Neurosci. 2002; 3:53–64. [PubMed: 11823805]

Weng S, Sun W, He S. Identification of ON-OFF direction-selective ganglion cells in the mouse retina. J Physiol. 2005; 562:915–923. [PubMed: 15564281]

Wojcik SM, Katsurabayashi S, Guillemin I, Friauf E, Rosenmund C, Brose N, Rhee JS. A shared vesicular carrier allows synaptic corelease of GABA and glycine. Neuron. 2006; 50:575–587. [PubMed: 16701208]

Yang G, Masland RH. Direct visualization of the dendritic and receptive fields of directionally selective retinal ganglion cells. Science. 1992; 258:1949–1952. [PubMed: 1470920]

Yang G, Masland RH. Receptive fields and dendritic structure of directionally selective retinal ganglion cells. J Neurosci. 1994; 14:5267–5280. [PubMed: 8083735]

Yoshida K, Watanabe D, Ishikane H, Tachibana M, Pastan I, Nakanishi S. A key role of starburst amacrine cells in originating retinal directional selectivity and optokinetic eye movement. Neuron. 2001; 30:771–780. [PubMed: 11430810]

Zheng JJ, Lee S, Zhou ZJ. A developmental switch in the excitability and function of the starburst network in the Mammalian retina. Neuron. 2004; 44:851–864. [PubMed: 15572115]

Zhou ZJ, Fain GL. Neurotransmitter receptors of starburst amacrine cells in rabbit retinal slices. J Neurosci. 1995; 15:5334–5345. [PubMed: 7623156]

Zhou ZJ, Lee S. Direction-Selective Light Responses of DS Ganglion Cells at the Onset of Vision. Invest Ophthalmol Vis Sci. 2005; 46:2242. [PubMed: 15980207]

Zhou ZJ, Lee S. Synaptic physiology of direction selectivity in the retina. J Physiol. 2008; 586:4371–4376. [PubMed: 18617561]

Zucker RS, Regehr WG. Short-term synaptic plasticity. Annu Rev Physiol. 2002; 64:355–405. [PubMed: 11826273]

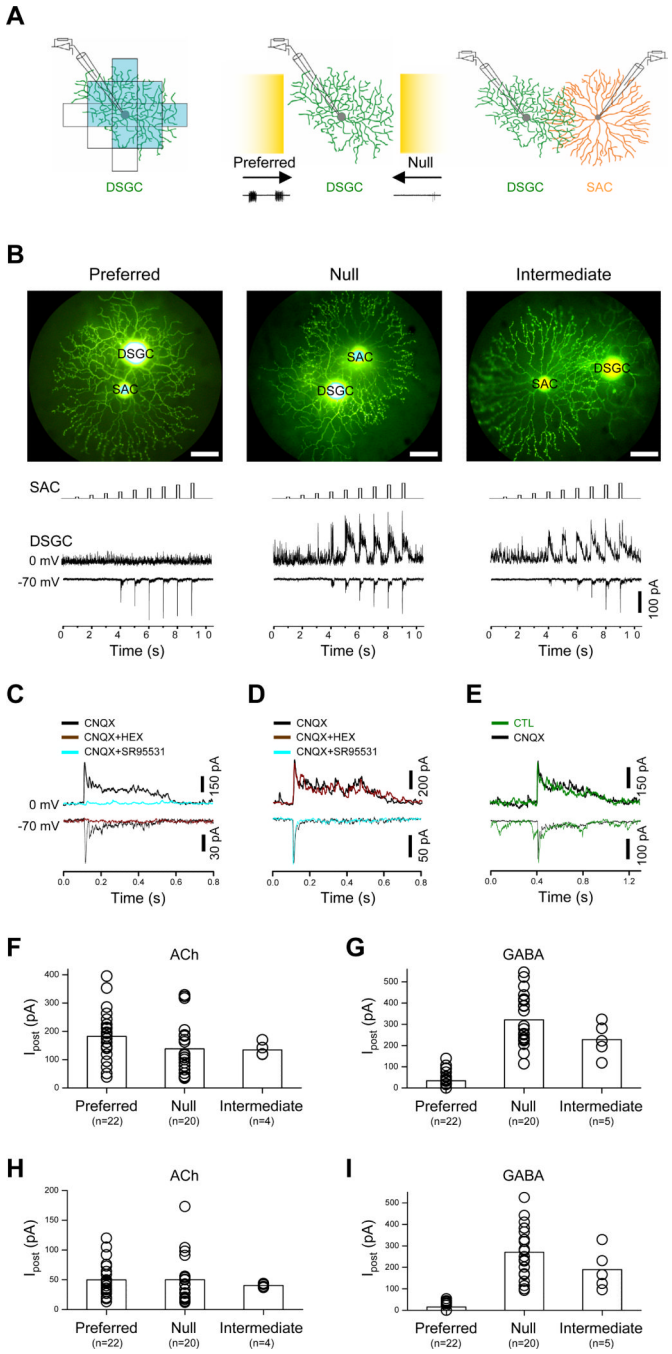

Figure 1. Symmetric cholinergic and asymmetric GABAergic synaptic connectivity between SAC and DSGC

A, Left-middle: Illustration of cell-attached recording from a DSGC showing the receptive field center (shaded in blue, mapped by a flashing a 80-μm×80-μm light spot in 13 locations), the preferred-null axis (indicated by arrows, identified by moving a 200-μm×600-μm light bar, shown in yellow, at 300 μm/s in 12 directions), and the spikes evoked by preferred and null movements (bottom traces). **Right:** Illustration of dual whole-cell recording from a DSGC and an overlapping SAC from the null direction. **B, Upper:** Photomicrographs of Lucifer yellow-filled SAC and DSGC pairs taken at the end of dual recordings, showing SACs located on the preferred (**left**), null (**middle**), and intermediate

(**right**) side of the DSGC (scale bar, 50 μm). **Lower:** Synaptic transmission from SACs to DSGCs, showing spatially symmetric inward postsynaptic currents at -70 mV (~E_{Cl}) and spatially asymmetric outward currents at 0 mV (~E_{Cat}) in responses to step depolarization of SACs in 10 mV amplitude increments from a holding potential of -70 mV, in the presence of 40 μM CNQX. **C,** Complete blockade of the outward postsynaptic currents by SR95531 (50 μM) and of the inward postsynaptic currents by hexamethonium (HEX, 200 μM). **D,** HEX (200 μM) did not block the evoked outward postsynaptic current at 0 mV, neither did SR95531 (50 μM) block the evoked inward postsynaptic current at -70 mV. **E**, CNQX (40 μM) blocked the majority of spontaneous excitatory postysynaptic currents in the DSGC, with no effect on the evoked inward or outward current inputs from the SAC. Statistical summary of the maximum (**F, G**) and first-detectable (**H, I)** amplitude of the inward (cholinergic) and outward (GABAergic) postsynaptic currents evoked by preferred-, null-, and intermediate side SACs under dual patch-clamp recording. Error bars: s.e.m.

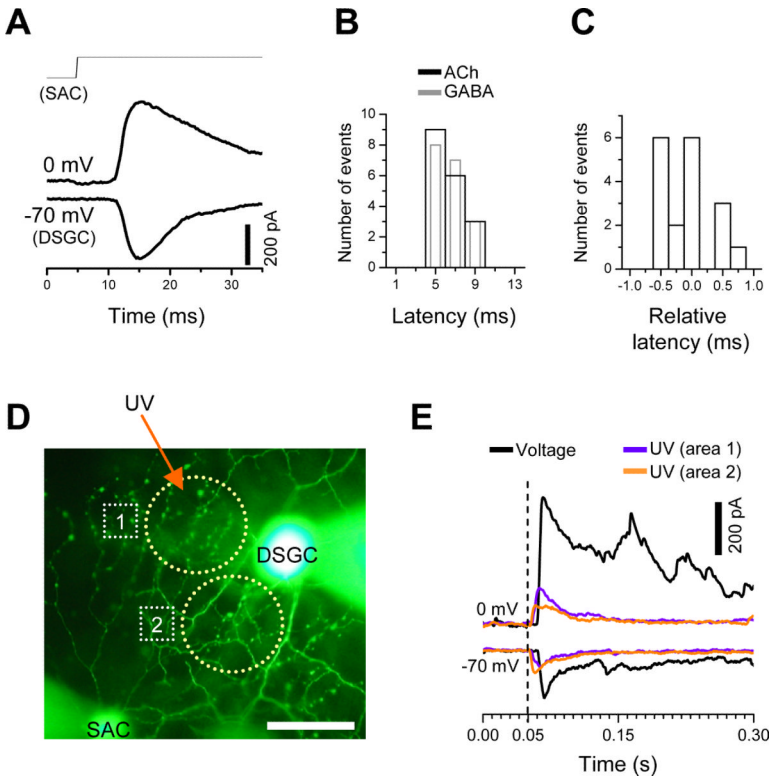

Figure 2. Monosynaptic cholinergic and GABAergic transmission between SAC and DSGC

A, Examples of synaptic transmission recorded from a SAC-DSGC pairs, showing that cholinergic (recorded at -70 mV) and GABAergic (recorded at 0 mV) transmissions could be evoked with a nearly identical delay following the step depolarization of SAC from -70 to 10 mV. **B,** Latency distribution of evoked postsynaptic currents, showing similar temporal delays between the onset of the presynaptic voltage pulse and the onset of postsynaptic cholinergic (black) and GABAergic (gray) currents. Data were pooled from eighteen different pairs. For clarity, the gray bars are shown with a reduced width, but the bin size (2 ms) is the same for both black and gray bars. **C,** Relative response latency, defined as the difference between the onset of GABAergic current and the onset of cholinergic current within the same paired recording, showing only submillisecond differences in response delay time. Eighteen different paired recordings were pooled. Bin size = 0.25 ms. **D,** Photomicrograph of a Lucifer yellow-filled SAC-DSGC pair (SAC on the Null side of the DSGC), showing two areas (yellow circle, 1 and 2) where a 50-μm-diameter UV spot was illuminated for 25 ms to uncage Ca^{2+} from DM-nitrophen (10 mM, preloaded with 80% Ca^{2+}) which was introduced to the SAC via the whole-cell patch pipette. The first UV illumination was given after 5 minutes after the establishment of a whole-cell configuration (scale bar, 50 μm). **E,** Postsynaptic cholinergic and GABAergic currents (recorded at -70 and 0 mV, respectively) evoked by a voltage step given to the SAC (from -70 to -20 mV, black traces) in Ames medium, and by UV photolysis (violet and orange traces) from the same SAC-DSGC pair after $CdCl_2$ (300 μM) was added to the bathing medium to block polysynaptic transmission. The onset of presynaptic step depolarization and the onset of UV illumination were aligned for clarity (broken vertical line). All traces were from the same SAC-DSGC pair in **D**.

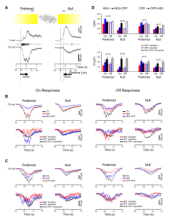

Figure 3. Contribution of cholinergic and GABAergic inputs to DSGC light responses

A, Responses of a DSGC to a moving light bar (yellow; the leading edge of bar started 900 μm away from DSGC soma and reached the soma at time = 0), showing spike responses to the leading edge of the bar (On responses) under loose cell-attached recording (middle traces), as well as IPSC (top traces, 0 mV) and EPSC responses (bottom traces, -70 mV) under whole-cell voltage-clamp recording. Red and blue dashed lines indicate the onset of the EPSC and IPSC, respectively. Distance axes indicate the location of the leading edge of the light bar corresponding to the time shown in Time axes. Drawings below the x-axes: dendritic diameter of the DSGC recorded. Only the On responses (to the leading edge of the moving light bar) were shown. **B,** Pharmacological components of the EPSCs (at -70 mV) in a DSGC evoked by the leading (On) and trailing edge (Off) of a moving light bar, showing in upper panels responses to preferred- and null-direction movements in the control (CTL) solution, followed by sequential applications of HEX (200-400 μM) and HEX (200-400 μM) + CPP (25 μM). Lower panels: isolated EPSC components obtained by subtracting currents recorded in HEX + CPP from those in HEX alone (CPP-sensitive component) and by subtracting currents recorded in HEX alone from those in CTL (HEX-sensitive component). **C,** Pharmacologically isolated EPSC components in a DSGC (at -70 mV) obtained by sequential application of CPP (25 μM) and CPP (25 μM) + HEX (200-400 μM). Traces in upper panels in **B**, **C** were averaged from two trials. **D**, Statistical analysis of the peak amplitude (upper panel) and the total charge transfer (lower panel) of the EPSC components from experiments exemplified in **B** and **C**, showing asymmetric HEX- and CPP-sensitive, but symmetric HEX-CPP-insensitive components in the preferred and null directions. Error bars: s.e.m. See also Figure S1.

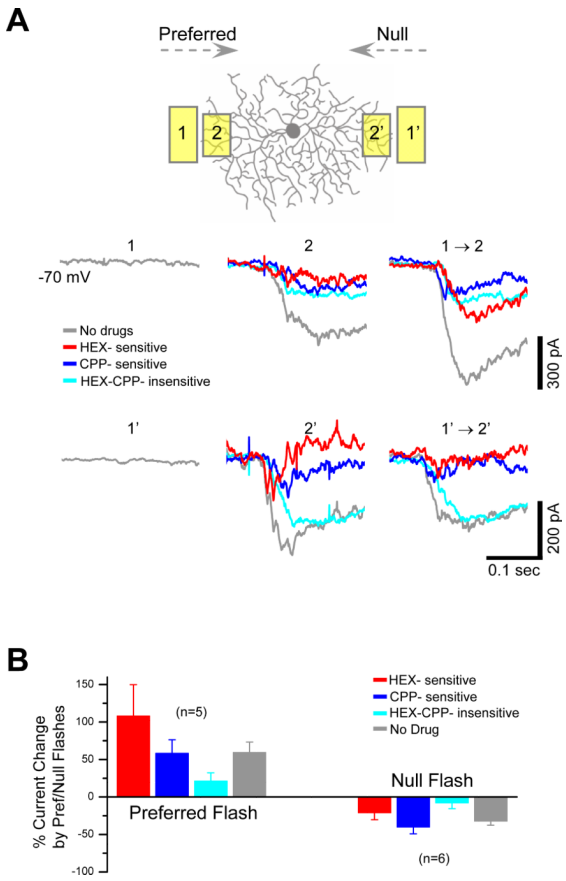

Figure 4. Directional facilitation and suppression of light-evoked, motion-sensitive cholinergic input to DSGCs

A, EPSC components during two-flash apparent motion in the preferred (1 to 2) and the null (1' to 2') direction. A conditioning light flash (1, 60-μm × 120-μm spot) on the preferred side immediately outside the cell's RF center evoked no response by itself, but greatly enhanced the subsequent response to a test light flash (2, 60-μm × 90-μm) within the RF center, indicating a motion-mediated facilitation of HEX- and, to a lesser degree, CPP-sensitive EPSC components in the preferred direction. Flashing the same conditioning light spot on the null side (1') also did not evoke a response by itself, but reduced the response to the subsequent test flash (2') located within the RF center, indicating a motion-mediated suppression of HEX- and CPP-sensitive EPSC components in the null direction. Traces were averaged from 2-4 trials. Spatial offset between conditioning and test flashes (center-to-center): 90 μm; temporal delay: 300 ms; apparent motion speed: 300 μm/s. **B,** Statistical analysis of the facilitation and suppression of the EPSC components during apparent motion, showing different degrees of motion sensitivity in different EPSC components. Error bars: s.e.m. See also Figure S2.

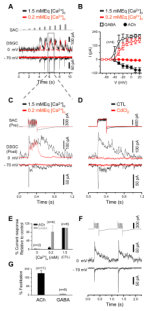

Figure 5. Differential regulation of ACh and GABA releases from SACs

A, Dual patch-clamp recording from a pair of SAC (null side) and DSGC, showing postsynaptic GABAergic (outward, at 0 mV) and cholinergic (inward, at -70 mV) responses recorded under normal (1.5 mMEq, black traces) and reduced (0.2 mMEq) extracellular calcium ($[Ca^{2+}]_o$) conditions. The cholinergic responses, but not the GABAergic responses, were completely abolished in 0.2 mMEq $[Ca^{2+}]_o$. The SAC was stimulated by depolarizing voltage pulses of increasing amplitudes (10 mV increments from -70 mV, top trace). **B,** Current-voltage relationship between the presynaptic depolarizing voltage and the corresponding postsynaptic current amplitude from experiments exemplified in **A**. **C,** Expanded view of presynaptic currents in the SAC and postsynaptic GABAergic (at 0 mV) and cholinergic (at -70 mV) responses in the DSGC for the depolarizing pulse (from -70 mV to -10 mV) marked by gray box in **A**. **D,** Complete blockade of cholinergic and GABAergic postsynaptic currents in a DSGC (evoked by depolarizing a SAC from -70 to 0 mV) by 300 μM $CdCl_2$. **E,** Summary of experiments exemplified in **C**, showing maximum cholinergic and GABAergic current amplitudes as a function of $[Ca^{2+}]_o$ (normalized by the control responses in 1.5 mM $[Ca^{2+}]_o$). **F,** Facilitation of cholinergic, but not GABAergic, synaptic transmission between SAC and DSGC by presynaptic pair-pulse stimulation from -70 to 0 mV. **G,** Summary of cholinergic and GABAergic facilitation by pair-pulse stimulation. Percent facilitation was defined as the increase in peak response amplitude (calculated by subtracting the peak amplitude of the first response from that of the second response), normalized by the first peak response amplitude. Error bars: s.e.m.

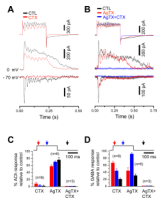

Figure 6. Effects of N and P/Q type Ca^{2+}-channel blockers on ACh and GABA release from SACs

A, ω-conotoxin GVIA (CTX, 1 μM) nearly completely abolished cholinergic responses, but only partially blocked GABAergic responses. **B,** ω-agatoxin IVA (AgTX, 500 nM) had a greater blocking effect on the peak GABA responses than did CTX, but it only partially blocked cholinergic responses. AgTX (500 nM) and CTX (1 μM) together blocked all cholinergic and GABAergic transmissions. **C, D,** Summary of effects of CTX and AgTX on the amplitude of evoked cholinergic (**A**) and GABAergic (**B**) responses at three different time points following the onset of presynaptic depolarization (red: 20ms, blue: 100ms, black: 300ms). The effects of CTX and AgTX were significantly different ($p<0.01$) on the ACh responses (at all three time points). They were also significantly different ($p<0.05$) on the GABA responses during the pulse (red and blue), but not after the pulse (black). CNQX (40 μM) was included in the superfusate for all recordings. Error bars: s.e.m.

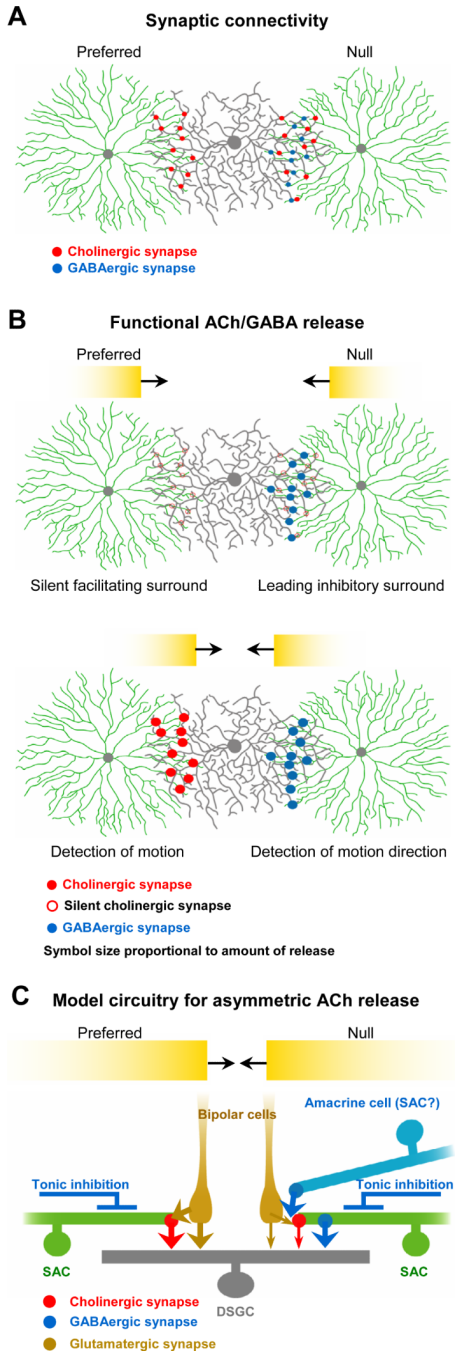

Figure 7. Role of ACh-GABA co-neurotransmission in motion- and direction-sensitivity

A, Anatomical connections between SAC and DSGC, showing symmetric cholinergic and asymmetric GABAergic synaptic connectivity (red and blue circles, respectively). ACh and GABA release sites are shown separately for clarity, but may in reality be located in close vicinity. Only those synapses that are formed with the DSGC shown in the center are illustrated. GABA release sites from the preferred SAC to other DSGCs are not shown. **B,** Functional properties of ACh and GABA releases by SACs during moving light stimulation. As light moves centrifugally from proximal to intermediate processes of a SAC, it produces in the distal dendrites an excitation that is sufficient to trigger GABA release from the distal processes, but not sufficient to trigger ACh release, resulting in a leading GABAergic lateral

inhibition (blue circles), but a “silent” cholinergic lateral excitation (hollow red circles). The leading GABAergic lateral inhibition, together with the asymmetric hardwiring shown in **A**, forms an asymmetric, spatially offset inhibition to produce direction selectivity in the DSGC. The “silent” cholinergic lateral excitation, on the other hand, facilitates the subsequent excitation at the distal SAC processes as the light further moves from intermediate to distal SAC dendrites, producing a motion-sensitive release of ACh (solid red circles) which is suited for detecting image motion. The “silent” nature of the cholinergic surround avoids the expansion of the DSGC RF center and creates motion-sensitivity without degrading spatial resolution. However, this facilitation occurs only at cholinergic synapses between SACs and DSGCs along the preferred direction; ACh release is suppressed by motion along the null direction by an additional mechanism, which likely involves direction-selective GABAergic inhibition at an upstream site. **C**, A parsimonious model of direction-selective inhibition of ACh release, showing SACs making cholinergic synapses (red) onto DSGC from both preferred and null directions, but making GABAergic synapses (blue) only from the null direction. The cholinergic synapses pointing in the null direction of the DSGC are suppressed from the null side by a GABAergic cell (most likely a SAC), which inhibits the cholinergic synapse either directly and/or via inhibition of bipolar cell axon terminals presynaptic to the SAC. This circuit is likely to involve additional GABAergic synapses, which are omitted here for simplicity. Furthermore, ACh release from both preferred and null directions is suppressed by a tonic GABAergic inhibition which greatly reduces the amplitude and spatial extent of the cholinergic surround to a DSGC. This model illustrates one of the many possible synaptic configurations that might explain the results observed.